Density functional study of single-wall and double-wall platinum nanotubes

Shyamal Konar* and Bikash C. Gupta†
Department of Physics, Visva-Bharati, Santiniketan 731235, India
(Received 11 May 2008; revised manuscript received 22 October 2008; published 8 December 2008)

The electronic structure calculations are carried out within the density functional formalism for understanding the structure and energetics of platinum nanotubes. Various single-walled platinum nanotubes (both chiral and achiral) and double-walled platinum nanotubes (only achiral) are considered here. Our calculations reveal that among six row strand nanotubes, the relaxed Pt(6,4) is most stable while among the five row strand nanotubes, the relaxed Pt(5,3) is most stable. After complete relaxation, the atomic structures of both the Pt(6,4) and Pt(5,3) nanotubes remain tubular and chiral. However, the initial chirality is not retained in the final atomic structure. The double-walled platinum nanotubes, namely, the Pt(6,6)@(13,13), Pt(5,5)@(12,12), Pt(4,4)@(11,11), and Pt(1,1)@(7,7) are studied. The atomic structures of these double-walled nanotubes remain double walled and tubular after complete relaxation. It is interesting to note that most of our results agree with the existing experimental results.

DOI: 10.1103/PhysRevB.78.235414 PACS number(s): 61.46.Fg, 73.63.Fg, 78.67.Ch

I. INTRODUCTION

After the invention of carbon nanotube (CNT) in 1991,[1] a new research area has emerged for the development of one-dimensional nanostructures, i.e., nanowires and nanotubes. Due to their fascinating physical and electronic properties, the nanowires and nanotubes constitute an important class in nanoelectronics with their huge potential application in nanoscale devices i.e, field-effect transistor (FET) nonlinear devices, nanotube sensors etc. They may also be used as interconnects in circuit devices.

It has been realized that nanowires and nanotubes of other materials may also be used for various technological applications. Therefore, the physics of nanowires, nanotubes of other materials and their formations are studied both experimentally and theoretically. For example, the nanotubes of Group-III nitrides, such as, BN, AlN, GaN,[2–4] and several other nanotubes, such as NiCl, $H_2Ti_3O_3$, TiO_2, SiC, and Si (Refs. 5–10) have been observed experimentally. Some important theoretical investigations have also been made on the nanowires and nanotubes. These include, the study on structural and electrical properties of several nanotubes such as C, Si, SiC, BeO, and BN,[11–21] and the study on the change in the functionality of nanotubes due to doping of various elements. In this context, it may be mentioned that the change in functionality of CNTs due to the doping of metal and nonmetal atoms[22,23] and that of Si nanotube due to the doping of transition metal[24] have extensively been studied.

The research on nanowires and nanotubes is not confined to carbon materials or composite materials or semiconducting materials. There have been some progress on the formation of nanowires and nanotubes composed of metal atoms such as gold, silver, and platinum.[25–35] The helical multishell (HMS) gold nanowire was first synthesized by Kondo *et al.*[33] in an UHV-TEM experiment. The gold nanowires are interesting due to their magic structures and conductances. The single-walled gold nanotube composed of five helical strands was found to exist in the UHV-TEM experiment conducted by Oshima *et al.*[34] An *ab initio* study of the evolution of physical and electronic properties of single-walled gold nanotubes was done by Senger *et al.* in 2004.[36] Based upon first-principles calculations, Elizondo *et al.* studied a variety of possible structure for single-walled silver nanotubes in 2006.[37]

In another experiment, Oshima *et al.*[38] showed the existence of the stable tip suspended HMS tubular platinum structure and the existence of single-walled platinum nanotube (SWPtNT). Platinum is known as an important metal with huge applications as catalyst for many important reactions. However, platinum tubes are expected to have a greater activity as catalyst compared to the ordinary platinum particle. This is due to the enhancement of catalytic activities associated with the convex surface of the inner wall of the tube. It is also conceivable that double-walled platinum nanotubes (DWPtNTs) should be more effective as catalyst compared to the SWPtNTs. The PtNT may also be used as possible interconnects in electronic nanodevices.

The above discussions suggest that an extensive theoretical study is essential for understanding the atomic structure, stability, and electronic properties of various platinum nanotubes. Another important aspect of such theoretical study is that a comparison of the theoretical results with the existing experimental results may enable us to conclude about the reproducibility of the nanotubes. An attempt was made to understand the atomic structure of a couple of single-walled platinum nanotubes only, namely, Pt(6,6) and Pt(5,5).[39] For completeness, we carry out an extensive theoretical study on various platinum nanotubes and compare the results with the experimental results whenever available. More specifically, our study includes the calculation of binding energies, curvature energies, and string tensions etc. for freestanding PtNTs.

We use the conventional notation to represent the single-walled platinum nanotubes, i.e., Pt(n,m), where n and m are integers. The single-walled nanotubes with $n=m$ are known as achiral nanotubes and those with $n>m$ are known as chiral nanotubes. The achiral platinum nanotubes that we consider here ranges from Pt(4,4) to Pt(17,17). Among many, we consider only a few chiral nanotubes, namely, Pt(4,3), Pt(5,4), Pt(5,3), Pt(6,5), Pt(6,4), and Pt(6,3). In addition, some simple double-walled platinum nanotubes are studied.

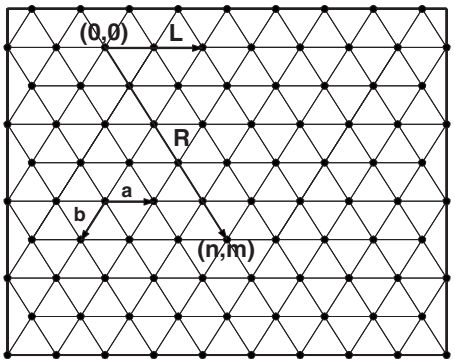

FIG. 1. The 2D triangular lattice network of Pt(111) sheet is shown here. The atomic structure of Pt(n,m) is obtained by cylindrical folding of Pt(111) sheet. The circumference (R) and unit cell length (L) are shown for the Pt(5,5) nanotube.

A simple double-walled platinum nanotube is composed of two single-walled nanotubes where a Pt(p,p) is enclosed within the Pt(q,q) and it is denoted as Pt(p,p)@(q,q). The double-walled platinum nanotubes that we consider in this paper are Pt(6,6)@(13,13), Pt(5,5)@(12,12), Pt(4,4)@(11,11), and Pt(1,1)@(7,7). However, Pt(1,1)@(7,7) is nothing but an atomic wire enclosed within a Pt(7,7) nanotube.

The paper is organized as follows. The formalism is given in Sec. II and the results and discussions are presented in Sec. III. Finally we summarize our findings in Sec. IV.

II. APPROACH AND METHOD

The crystal lattice structure of the platinum bulk is face-centered cubic with lattice constant (bond length) 3.92 Å (2.77 Å). The Pt(111) atomic sheet, extracted from platinum bulk, has a closely packed two-dimensional (2D) triangular lattice structure as shown in Fig. 1. The single-walled platinum nanotube Pt(n,m) can be constructed by wrapping the Pt(111) atomic sheet onto the surface of a cylinder of radius r. The chiral vector $\vec{C}=n\vec{a}+m\vec{b}$ is such that the circumference (R) and the radius (r) of the tube are $R=|\vec{C}|$ and $r=\sqrt{(n^2+m^2-nm)}|\vec{a}|/2\pi$, respectively. Here, $\vec{a}$ and $\vec{b}$ are the basis vectors of the 2D Pt(111) sheet. The unit cell length (L) of the tube is $|\vec{L}|$ where $\vec{L}$ is the unit cell length vector. The DWPtNTs are formed by rolling two planer Pt (111) sheets with a common axis.

To obtain the minimum energy structures of the SWPtNTs and DWPtNTs, we carry out total energy calculations within the density functional theory at zero temperature. The VASP code is used for this purpose.[40–42] The wave functions are expressed by plane waves with the cutoff energy $|k+G|^2 \leq 350$ eV. The Brillouin zone (BZ) integrations are performed by using the Monkhorst-Pack scheme with $1\times1\times40$ k-point meshes for a primitive cell. The convergence criterion for energy is considered to be less than 10^{-5} eV. All the calculations are performed in a periodically repeating supercell. The supercell size is taken to be 30 Å$\times$30 Å$\times n_{\text{cell}}L$ to avoid interaction of a tube with its image

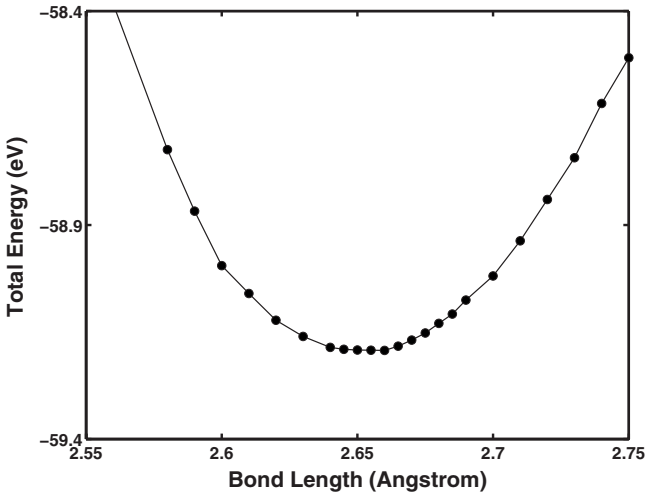

FIG. 2. Total energy per supercell is plotted as a function of the Pt-Pt bond length of the achiral Pt(6,6) nanotube. The optimal bond length turns out to be 2.66 Å.

where n_{cell} is the number of the unit cell of the platinum nanotube. The convergence is achieved with the above parameters. Ions are represented by ultrasoft Vanderbilt-type pseudopotentials[43] and results for fully relaxed atomic structures are obtained using the generalized gradient approximation (GGA). The preconditioned conjugate gradient method is used for the wave function optimization and the conjugate gradient method for ionic relaxation. All the atoms in the supercell are assumed to reach the relaxed positions when the force on each atom is less than 0.01 eV/Å. Note that the spin polarized calculations are done for obtaining the total energy of a platinum nanotube. In addition, for comparison, all the calculations for the single-walled platinum nanotubes are also done using the PAW potential within the VASP.

III. RESULTS AND DISCUSSIONS

First, it is necessary to determine the optimum lattice constant of a PtNT. For that purpose, one needs to determine the optimal Pt-Pt bond length by calculating the total energy of a nanotube by varying the Pt-Pt bond length. We have performed the calculations for obtaining the optimal lattice constants of all the PtNTs considered here. The total energy with respect to the bond length for Pt(6,6) and Pt(6,5) tubes are shown in Figs. 2 and 3, respectively. From Figs. 2 and 3 we find that the optimal bond length for the Pt(6,6) tube is $\approx$2.66 Å while that for the Pt(6,5) tube is $\approx$2.60 Å. Also note that for all the chiral PtNTs [Pt(6,5), Pt(6,4), Pt(6,3), Pt(5,4), Pt(5,3), and Pt(4,3)] the optimal bond length is $\approx$2.60 Å and for the achiral PtNTs the optimal bond length is $\approx$2.66 Å. We also note that the optimal Pt-Pt bond length for 2D Pt(111) sheet is $\approx$2.73 Å.

Once the optimal Pt-Pt bond length and, hence, the optimal lattice constant of a PtNT are obtained, we allow all the Pt atoms in the tube to relax completely. After the complete relaxation, the total binding energy, E_{BE}, of a PtNT is obtained from the expression: $E_{\text{BE}}=-[(E_{\text{total}}(\text{PtNT})-NE_{\text{atomic}}(\text{Pt})]$ where, $E_{\text{total}}(\text{PtNT})$ represents the total en-

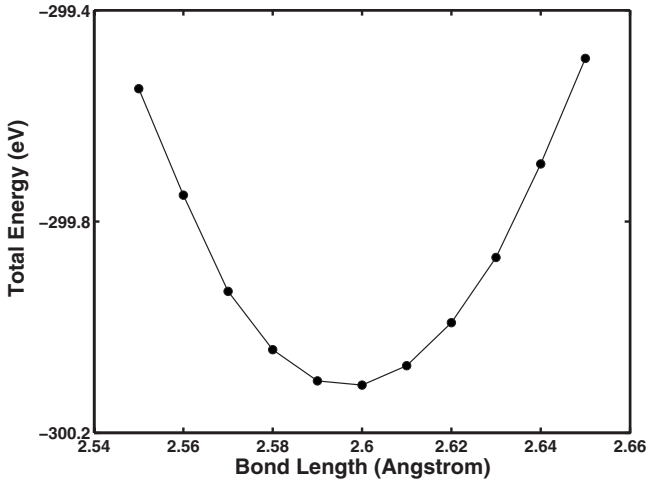

FIG. 3. Total energy per super cell is plotted as a function of the Pt-Pt bond length of the chiral Pt(6,5) nanotube. The optimal bond length turns out to be 2.60 Å.

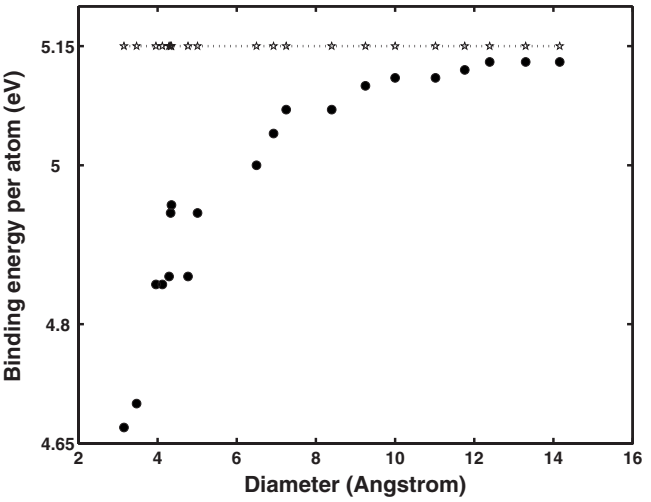

FIG. 4. This shows the variation in binding energy per atom with diameter for several single-walled platinum nanotubes. The dotted line corresponds to the binding energy per atom for 2D Pt(111) sheet. Notice that the binding energy per atom for single-walled nanotubes in the larger diameter regime approaches toward the value of the binding energy per atom for the 2D Pt(111) sheet.

ergy of the relaxed PtNT consisting of N platinum atoms within the supercell and $E_{\text{atomic}}(\text{Pt})$ represents the atomic energy associated with an isolated Pt atom.

A positive value of E_{BE} indicates a local or a global minima of the Born-Oppenheimer surface which generally corresponds to a stable structure. Again, from the E_{BE}, one may calculate the curvature energy [the energy required to form a one-dimensional tubular structure by folding the 2D triangular Pt(111) sheet] in order to have the mechanical insight of a PtNT. The curvature energy per atom, E_c, can easily be calculated by using the formula, $E_c=[E_{\text{BE}}(\text{sheet})-E_{\text{BE}}(\text{PtNT})]/N$, where $E_{\text{BE}}(\text{sheet})$ represents the total binding energy of the 2D Pt(111) sheet consisting of N platinum atoms and $E_{\text{BE}}(\text{PtNT})$ represents the total binding energy associated with the tube constructed from the same Pt sheet. We have calculated the binding energy per platinum atom for the two-dimensional platinum sheet and it is ≈ 5.15 eV. All the results for SWPtNTs and DWPtNTs are presented in subsequent subsections.

A. Single-wall platinum nanotubes

Figure 4 illustrates the binding energy per platinum atom (E_{BE}/atom) of the single-walled platinum nanotubes as a function of diameter. It is clear from Fig. 4 that the E_{BE}/atom increases as the diameter (D) of the tube increases. This trend is quite logical because larger strain is induced for the smaller diameter tubes. In the larger diameter region, the E_{BE}/atom tends to saturate toward the value of 5.15 eV. Therefore, one expects that the E_{BE}/atom for a tube with infinite diameter should be 5.15 eV which is consistent with the value calculated for the 2D Pt(111) sheet. Note that the binding energy calculations by the use of PAW potential reflect the similar behavior (see Tables I and II).

The curvature energies of the single-walled platinum nanotubes are plotted as a function of the inverse square of the diameter of the nanotubes and this is shown in Fig. 5. It is clear from Fig. 5 that the curvature energy/atom (E_c in eV) decreases with the increase in diameter of the SWPtNTs. The expression of E_c obtained from classical elasticity theory is $E_c=Y\omega^3\Omega/24r^2$ (Y: Young's modulus, ω: thickness of the nanotube, and Ω: atomic volume) (Ref. 36) when the tubes are perfectly cylindrical. It is interesting to note that even though the relaxed SWPtNTs (we will see in the later part of our discussions that the relaxed SWPtNTs are not perfectly cylindrical) are not perfectly cylindrical, yet the graphical plot of E_c vs $1/D^2$ is a straight line and it fits closely with $E_c=\alpha/D^2$ where the value of α is approximately 5.30 eV Å^2 (see Fig. 5). Thus, the trend of our results satisfy the theoretical variation in curvature energy with diameter and it reflects the mechanical behavior similar to that of a carbon nanotube.

As far as the stability of the tubes is concerned, the comparison of the E_{BE} per atom of the tubes is not sufficient to conclude about the physical stability of the tubes. In fact, our calculations are done for infinitely extended nanotubes, while the nanotubes fabricated in experiments are finite and stretched between two platinum electrodes. Naturally an apparent contradiction appears between the theory and the experiment. Hence, E_{BE} per atom should not be taken as a sufficient criterion to decide on the long lived metastable states of suspended nanotubes and nanowires. It is therefore more physical to introduce the criterion of minimum string tension[36] rather than the total free energy for the stability of nanowire or nanotube. Here, we carry out the string tension analysis for all the platinum nanotubes. The string tension of a nanowire (nanotube) is defined as positive work done in drawing the wire (tube) out of the tips and is given by $f=(F-\mu N)/L$, where F is the total free energy, μ is the chemical potential of platinum in the bulk, and L is the length of the tube within the supercell. The free energy, F, is the total cohesive energy at zero entropy and this is given as $[E_{\text{total}}(\text{PtNT})-NE_{\text{atomic}}(\text{Pt})]$ for a nanotube consisting of N atoms within the supercell. The bulk chemical potential of platinum is calculated and its value is ≈ -5.96 eV.

TABLE I. Various physical quantities of the relaxed single-walled platinum nanotubes (achiral nanotubes only) are given.

Pt nanotube	E_{BE}/atom (eV)	Curvature energy/atom (eV)	Diameter (theor.) (Å)	Diameter (expt.) (Å)	String tension (eV/Å)	Average width (Å)	E_{BE}/atom (eV) (PAW calc.)
Pt(4,4)	4.70	0.45	3.47		2.20	3.41	4.75
Pt(5,5)	4.86	0.30	4.29		2.42	4.13	4.90
Pt(6,6)	4.94	0.21	5.01	4.80	2.68	4.96	4.98
Pt(7,7)	5.00	0.145	6.50		2.93	5.32	5.05
Pt(8,8)	5.04	0.115	6.93		3.25	6.68	5.09
Pt(9,9)	5.07	0.079	7.25		3.52	7.10	5.11
Pt(10,10)	5.07	0.080	8.40		3.92	8.39	5.12
Pt(11,11)	5.10	0.055	9.25		4.18	9.01	5.15
Pt(12,12)	5.11	0.045	10.00		4.50	9.85	5.15
Pt(13,13)	5.11	0.044	11.02		4.88	10.96	5.16
Pt(14,14)	5.12	0.027	11.76		5.14	11.59	5.16
Pt(15,15)	5.13	0.02	12.39		5.48	12.28	5.18
Pt(16,16)	5.13	0.015	13.30		5.84	13.20	5.18
Pt(17,17)	5.13	0.010	14.16		6.20	14.09	5.19

The string tension curve in Fig. 6 shows a few minima compared to their immediate neighboring structures. As for the single-walled platinum nanotubes there are only two minima, one corresponds to the relaxed Pt(6,4) and other corresponds to the relaxed Pt(5,3). Also note that the string tension curve obtained for the single-walled nanotubes by the use of PAW potential is shown in Fig. 7 and it reflects similar behavior as in Fig. 6. In high resolution transmission electron microscope (HR-TEM) experiment, the diameter of 4.8 Å and the apparent width in the range of 4.0 to 4.6 Å have been measured[38] for single-walled platinum nanotubes with six row strands. Now the questions are: which Pt nanotube with six row strands becomes most stable after complete relaxation and how robust the experimental results are? Our results confirm from different directions that among the nanotubes with six row strands, the Pt(6,4) becomes most stable after full relaxation. In one hand, the Pt(6,4) corresponds to a minimum in the string tension curve and consequently, the relaxed Pt(6,4) belongs to a magic structure. On the other hand, by comparing the binding energy per atom among the nanotubes with six row strands, we find that the relaxed Pt(6,4) is energetically more favorable over the relaxed Pt(6,6), Pt(6,5), and Pt(6,3) by 0.01, 0.09, and 0.01 eV, respectively. The results obtained from our calculations for average width and diameter of the relaxed Pt(6,4) nanotube are approximately 4.0–4.3 Å and 4.35 Å, respectively, and these results more or less agree with the experimental results.[38] Note that the average width of a nanotube is measured by taking the projection of the tube on a plane parallel to the cylindrical axis of the nanotube and the average diameter of a nanotube is measured by taking the projection of the nanotube on a plane perpendicular to the axis of the nanotube.

All the nanotubes with six row strands remain hollow after complete relaxation. For example, the hollowness (central region with no charge density) of the relaxed Pt(6,4) is visible in the Fig. 8 where the total charge density is plotted in a plane perpendicular to the axis of the tube. Though the relaxed Pt(6,3), Pt(6,4), and Pt(6,5) remain chiral in nature, their initial well-defined chirality is lost. For the relaxed Pt(6,6) nanotube, the alternate hexagons along the tube axis are almost identical in structure. However, the consecutive

TABLE II. Various physical quantities of the relaxed single-walled platinum nanotubes (chiral nanotubes only) are given.

Pt nanotube	E_{BE}/atom (eV)	Curvature energy/atom (eV)	Diameter (theor.) (Å)	Diameter (expt.) (Å)	String tension (eV/Å)	Average width (Å)	E_{BE}/atom (eV) (PAW Cal.)
Pt(6,5)	4.86	0.290	4.77	4.80	2.67	4.44–4.54	4.90
Pt(6,4)	4.95	0.205	4.35	4.80	2.36	4.00–4.30	4.99
Pt(6,3)	4.94	0.200	4.33	4.80	2.37	4.15	4.97
Pt(5,4)	4.85	0.299	4.12		2.14	4.00	4.90
Pt(5,3)	4.85	0.300	3.96		2.09	3.80	4.89
Pt(4,3)	4.67	0.474	3.15		2.00	3.10	4.72

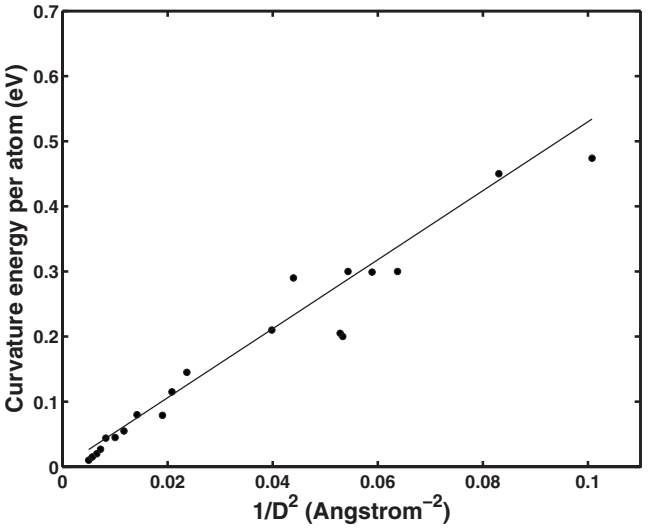

FIG. 5. The curvature energy per atom is plotted for single-walled platinum nanotubes as a function of $1/D^2$. Dotted line is the best fit for the curvature energy per atom versus $1/D^2$ plot.

hexagonals have different diameters. The distance between two consecutive hexagons is around 2.28 Å. The distribution of the Pt-Pt bond lengths of the relaxed Pt(6,6), Pt(6,5), Pt(6,4), and Pt(6,3) are shown in Table III. From Table III, we note that for the most favorable nanotube among the nanotubes with six row strands [i.e., Pt(6,4)] the fluctuation in bond length around the mean bond length is much less compared to that of the Pt(6,6), Pt(6,5), and Pt(6,3). The atomic structure of the relaxed Pt(6,4) is shown in Fig. 9. To understand the electrical nature of the Pt(6,4), we have plotted the density of states as a function of energy (see Fig. 10). The finite number of electronic density of states of Pt(6,4) around fermi energy clearly indicates that the tube is metallic in nature and therefore, it may be used as metallic interconnects in circuit devices.

The binding energies per atom for the relaxed nanotubes with five row strands [i.e., Pt(5,3), Pt(5,4) and Pt(5,5)] are

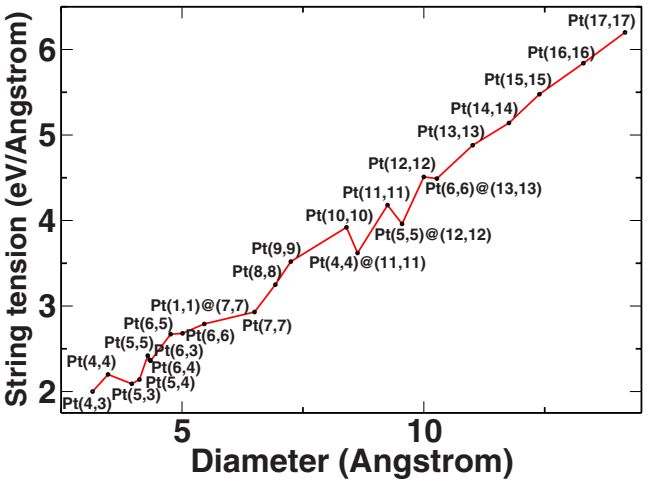

FIG. 6. (Color online) String tension values are plotted as a function of diameter of the single-walled and double-walled platinum nanotubes.

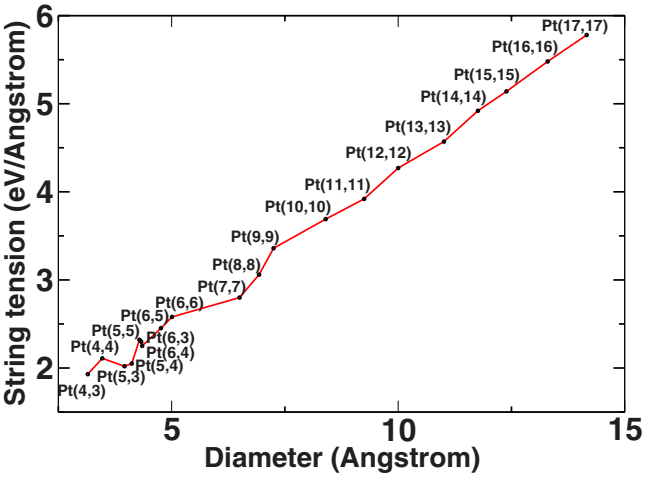

FIG. 7. (Color online) String tension values are plotted as a function of diameter of the single-walled platinum nanotubes. Here, the PAW potential is used under the VASP.

very close to each other. However, from the string tension curve in Fig. 6 we observe that the relaxed Pt(5,3) belongs to a local minima. Therefore, among the nanotubes with five row strands, the relaxed Pt(5,3) is the most favorable one. In this context, it is worth mentioning that the Au(5,3) nanotube was found to be most stable.[36] All the relaxed nanotubes with five row strands remain hollow after complete relaxation. The hollowness of a nanotube may be observed from a charge density plot in a plane perpendicular to the axis of the tube. For example, see Fig. 11 where the total charge density is plotted for the Pt(5,3). The absence of charge in the central region indicates the hollowness of the nanotube. It should be noted that like the Pt(6,3), Pt(6,4), and Pt(6,5) nanotubes, the Pt(5,3) and Pt(5,4) remain chiral after complete relaxation but the initial well-defined chirality is not retained. The width and the diameter of Pt(5,3) nanotube are calculated by us and the values are ≈3.8 and ≈3.96 Å, respectively. Our

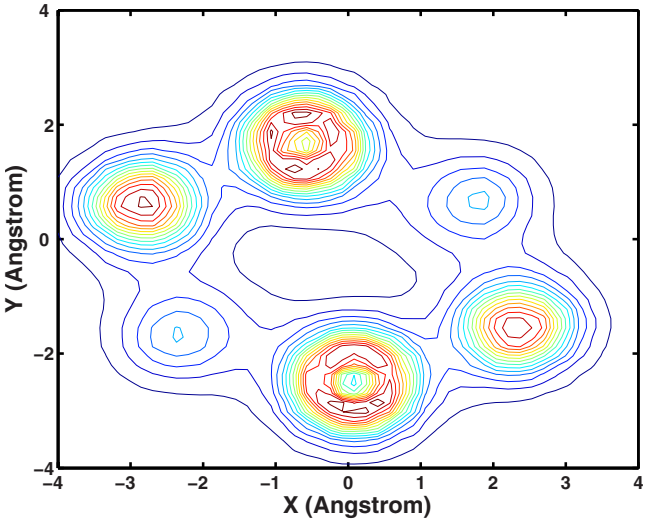

FIG. 8. (Color online) The total charge density plot of the Pt(6,4) nanotube on a plane perpendicular to the axis of the nanotube.

TABLE III. The bond length distributions of the relaxed single-walled platinum nanotubes are given.

Platinum nanotube	Minimum bond length (Å)	Maximum bond length (Å)	Mean (Å)	Standard deviation (Å)
Pt(4,4)	2.62	2.71	2.67	0.035
Pt(4,3)	2.58	2.76	2.64	0.043
Pt(5,5)	2.59	2.74	2.68	0.054
Pt(5,4)	2.55	2.74	2.67	0.045
Pt(5,3)	2.65	2.71	2.68	0.024
Pt(6,6)	2.52	2.73	2.65	0.075
Pt(6,5)	2.47	2.89	2.61	0.085
Pt(6,4)	2.60	2.72	2.66	0.035
Pt(6,3)	2.56	2.79	2.66	0.058
Pt(7,7)	2.54	2.76	2.66	0.079
Pt(8,8)	2.53	2.76	2.64	0.064
Pt(9,9)	2.56	2.83	2.64	0.059
Pt(10,10)	2.59	2.67	2.64	0.025
Pt(11,11)	2.54	2.67	2.61	0.026
Pt(12,12)	2.55	2.75	2.63	0.047
Pt(13,13)	2.58	2.67	2.62	0.025
Pt(14,14)	2.55	2.70	2.63	0.054
Pt(15,15)	2.55	2.62	2.63	0.085
Pt(16,16)	2.60	2.71	2.65	0.028
Pt(17,17)	2.58	2.70	2.65	0.036

results almost agree with the values (width: 3.5 Å and diameter: 4.1 Å) obtained by Oshima *et al.*[38] The Pt(5,3) nanotube may also be used as metallic interconnects in circuit devices because it shows finite density of states around the fermi energy [see Fig. 12 where the density of states are plotted as a function of energy for Pt(5,3)].

The relaxed Pt(5,5) nanotube consists of irregular pentagons with variable diameter. The distance between two consecutive pentagons is approximately around 2.30 Å. The distribution of the Pt-Pt bond length of the relaxed Pt(5,5), Pt(5,4), and Pt(5,3) is shown in Table III. We observe that the mean bond lengths for the relaxed Pt(5,3), Pt(5,4), and Pt(5,5) are around 2.68 Å. The distribution of bond length of the most stable one among the nanotubes with five row strands [i.e., Pt(5,3)] has a sharp peak at 2.70 Å, and the fluctuation about the mean bond length is very small. This kind of sharp peak at a particular bond length was also found for Au(5,3) nanotubes.[36] The relaxed atomic structure of the Pt(5,3) is shown in Fig. 13. The Pt(5,3) nanotube is yet to be

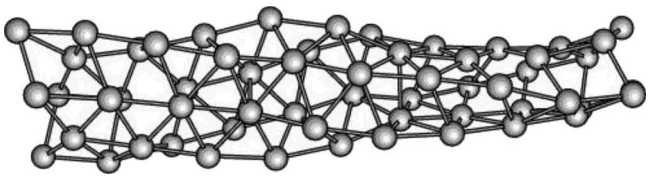

FIG. 9. The relaxed atomic structure of the chiral Pt(6,4) nanotube within one unit cell is shown.

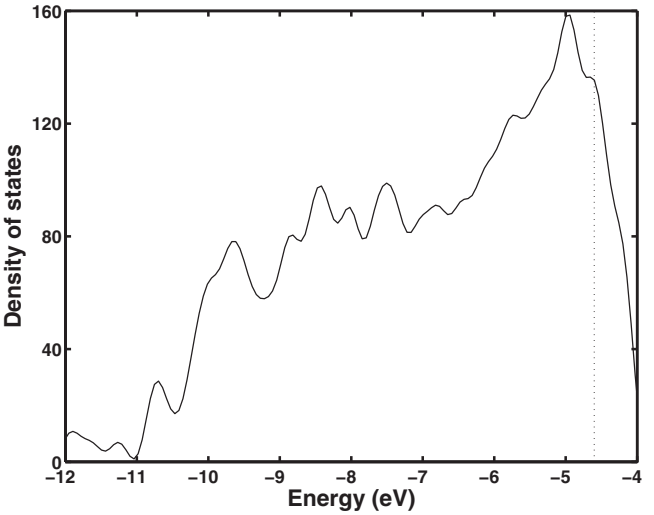

FIG. 10. Electronic density of states (DOS) are plotted as a function of energy for the Pt(6,4) nanotube. The vertical line (dotted) indicates the fermi energy level.

observed experimentally. It may be done by peeling off the outer shell of Pt(5,5)@(12,12).

Among the nanotubes with four row strands the Pt(4,3) corresponds to a lower string tension value compared to the Pt(4,4). Both the Pt(4,3) and Pt(4,4) remain hollow and tubular after complete relaxation. The Pt(4,3) remain chiral in nature. The cross section of the relaxed Pt(4,4) shows a square structure and the distance between two consecutive squares is ≈2.29 Å. The distribution of bond lengths of Pt(4,4) and Pt(4,3) are shown in Table III. The atomic structures of the relaxed Pt(7,7), Pt(15,15), and Pt(17,17) are irregular septagonal, hollow, and tubular. The relaxed Pt(8,8), Pt(14,14), and Pt(16,16) nanotubes have irregular octagonal and hollow tubular structure. The relaxed Pt(9,9) consists of irregular quadrilaterals. It has hollow and tubular structure with the average diameter ~7.25 Å. The atomic structure of

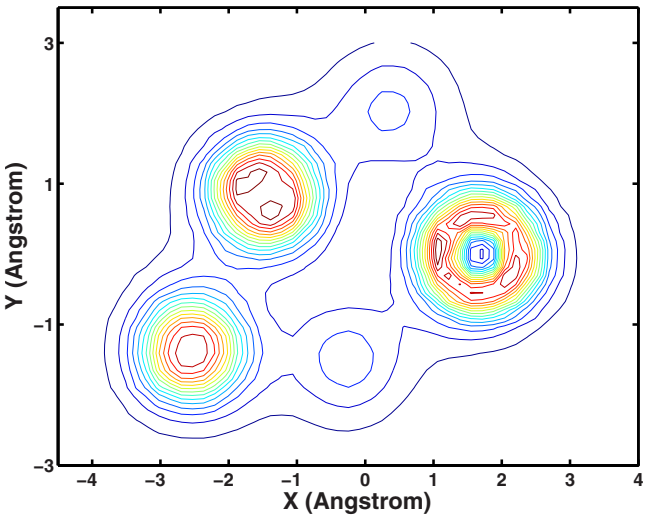

FIG. 11. (Color online) The total charge density of the Pt(5,3) nanotube is plotted on a plane perpendicular to the axis of the nanotube.

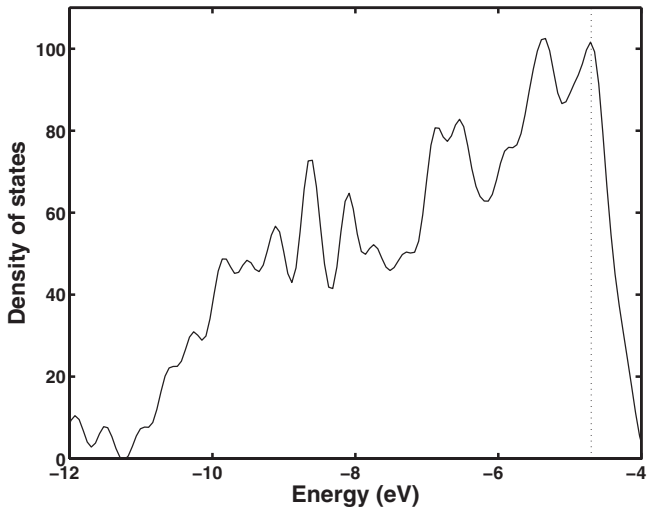

FIG. 12. Electronic density of states versus energy plot of the Pt(5,3) nanotube. The vertical line (dotted) indicates the fermi energy level.

relaxed Pt(10,10) is almost circular, hollow, and tubular with the average diameter ≈8.40 Å. The atomic structure of the relaxed Pt(11,11) is hollow and tubular with average diameter ≈9.25 Å. The relaxed Pt(12,12) and Pt(13,13) nanotubes are composed of irregular hexagons and they are hollow and tubular in structure with average diameter ≈10.00 and ≈11.02 Å, respectively. The statistical analysis of the Pt-Pt bond lengths for all the nanotubes (that we have discussed so far) are shown in Table III. Table III clearly shows that the values of mean Pt-Pt bond lengths of all the nanotubes range from 2.61 to 2.68 Å. Among all the single-walled platinum nanotubes, the relaxed Pt(10,10) retains a beautiful cylindrical structure with almost uniform diameter of ≈8.40 Å along the tube axis is shown in Fig. 14. This particular tube may be very useful for technological and medical purposes.[44] Therefore, more experiments should be performed in search of Pt(10,10) nanotube.

Finally, we note that the stable single-walled platinum nanotubes predicted from our calculations are relaxed Pt(6,4) and Pt(5,3). These are chiral in nature and therefore they are of special interest due to the possibility of having chiral currents along the helical strand and consequently they may have self-inductance and nanocoil effects.

B. Double-walled platinum nanotubes

The double-walled platinum nanotubes that we consider here consists of two concentric achiral single-walled platinum nanotubes. For the initial configurations, Pt-Pt bond

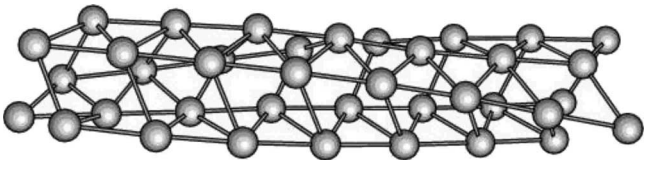

FIG. 13. The relaxed atomic structure of the chiral Pt(5,3) nanotube within one unit cell is shown.

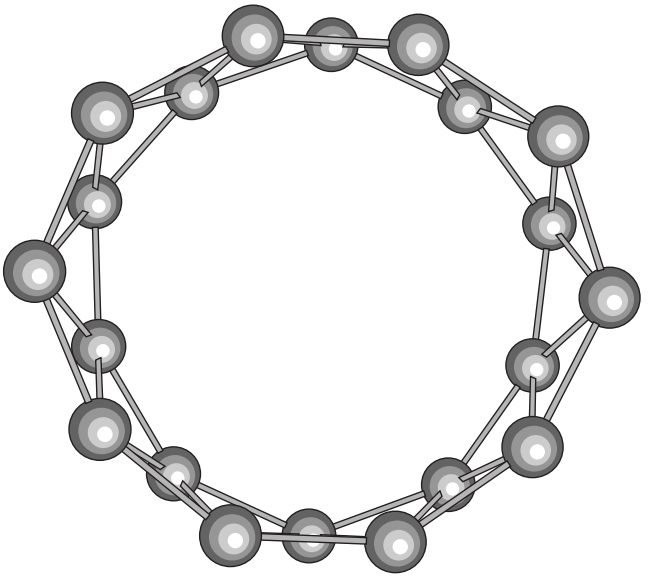

FIG. 14. The relaxed atomic structure of the achiral Pt(10,10) nanotube within one unit cell is shown.

length is considered to be 2.66 Å. All the relevant quantities such as binding energy per atom, string tension, inner and outer diameters, and average width of all the relaxed double-walled platinum tubes are summarized in Table IV. However, first, we discuss about the Pt(6,6)@(13,13) nanotube. The binding energy per atom of the fully relaxed Pt(6,6)@(13,13) is ~5.42 eV which is larger when compared with Pt(6,6) and Pt(13,13). Therefore, one may argue that for the free-standing nanotubes, the double-walled platinum nanotubes are more favorable compared to the single-walled platinum nanotubes. The average width and outer diameter of Pt(6,6)@(13,13) obtained from our calculation are ≈9.90 and ≈10.27 Å, respectively. The apparent width of Pt(6,6)@(13,13) obtained by us is almost close to the experimental result (width=9.8 Å) obtained by Y. Oshima *et al.*[38] After complete relaxation, the Pt(6,6)@(13,13) remains double walled and the inner and the outer shells are clearly distinguished. This is clearly seen in Fig. 15 where the total charge density is plotted on a plane perpendicular to the axis of the Pt(6,6)@(13,13) tube. The distributions of bond length of the inner and outer shells are 2.61–2.78 Å and 2.57–2.72 Å, respectively. To understand the nature of bonding between the inner-shell atom and the outer-shell atom, the charge density is plotted along a line joining two atoms, one from the inner shell and the other from the outer shell. This is shown in Fig. 16. It is clear from Fig. 16 that the bondings between the inner-shell atom and the outer-shell atom are mostly covalent in nature.

In the recent experiment, the Pt(6,6)@(13,13) was used to obtain the single-walled platinum nanotube with six row strands. It is done by peeling off the outer shell of some portion of the Pt(6,6)@(13,13) nanotube. Once the inner tube of Pt(6,6)@(13,13) was exposed, the width of the exposed inner tube was measured along the tube axis. It was observed that the exposed inner tube with six row strands shows a width of 4.0 Å, however, a larger width was observed at a point which is closer to the unpeeled portion of the

TABLE IV. Various physical quantities of the relaxed double-walled platinum nanotubes are given. The result within the first bracket is experimental.

Pt nanotube	Cell length (Å)	E_{BE}/atom (eV)	Average diameter in tube (Å)	Average diameter out tube (Å)	String tension (eV/Å)	Average width (Å)
Pt(6,6)@(13,13)	9.12	5.418	5.24	10.27	4.49	9.90 (9.80)
Pt(5,5)@(12,12)	9.14	5.428	5.10	9.55	3.96	9.06
Pt(4,4)@(11,11)	9.17	5.406	4.34	8.63	3.62	8.35
Pt(1,1)@(7,7)	9.11	5.166	0.00	5.46	2.79	5.14

Pt(6,6)@(13,13) platinum nanotube.[38] In our calculations, the results of the width and diameter of the inner shell of Pt(6,6)@(13,13) are more than that of the relaxed single-walled Pt(6,6) and it supports the experimental observation.[38] The increase in the width and diameter of the inner shell of Pt(6,6)@(13,13) is due to the interaction of the outer shell atoms with the inner shell atoms.

As the Pt(6,6)@(13,13) tube has a total of 19 row strands, one may expect that 19 channels would be available for conduction. However, taking effects of *d* electrons into account, the conductance for the Pt(6,6)@(13,13) may be more than $19G_0$ where $G_0=\frac{2e^2}{h}$ is unit quantum conductance. The band structure plot in Fig. 17 clearly shows that nine bands are crossing the Fermi level and therefore, the tube is metallic in nature with an approximate conductance of $9G_0$. This clearly indicates that some channels are suppressed due to the interaction of the inner shell atoms with the outer shell atoms. In recent studies it is found that unlike the case of gold atomic chain, a single infinite chain of platinum atoms has variable conductances.[45] The value of conductances of monoatomic infinite chain of Pt varies from $1G_0$ to $1.6G_0$ (the effect of *d* electrons in addition to *s* electron). Hence, in practice, the conductance of Pt(6,6)@(13,13) may be larger than $9G_0$.

We next, consider the Pt(5,5)@(12,12) nanotube which is of great interest from experimental point of view. The Pt(5,5)@(12,12) is first completely relaxed and then the average width and outer shell diameter of the nanotube is measured. They are ≈9.06 and ≈9.55 Å, respectively. Our values for the average width and the outer shell diameter almost agree with the results (width: 8.6–8.9 Å, diameter: 9.3 Å) obtained by Oshima *et al.*[38] for the Pt(5,5)@(12,12) nanotube. The atomic structure of the relaxed Pt(5,5)@(12,12) remains double walled, hollow, and tubular. The diameter of the inner shell (~5.10 Å) of the Pt(5,5)@(12,12) is more than the diameter of the relaxed single-walled Pt(5,5) [4.29 Å] and this is due to the interaction of the atoms of inner shell with the atoms of the outer shell. The Pt-Pt bond lengths of the relaxed Pt(5,5)@(12,12) ranges from 2.59 to 2.85 Å.

The next possible double-walled platinum nanotube which may experimentally be observed and may be useful for extracting the single-walled Pt(4,4) nanotube is Pt(4,4)@(11,11). The average width and the outer shell diameter obtained from our calculations for the relaxed Pt(4,4)@(11,11) are ≈8.35 and ≈8.63 Å, respectively. Our results almost agree with the values (width: 7.8–8.2 Å, outer shell diameter: 8.5 Å) obtained by Oshima *et al.*[38] The atomic structure of the relaxed Pt(4,4)@(11,11) remains double walled, hollow, and tubular with the Pt-Pt bond lengths ranging from 2.59 to 2.72 Å. Here also the average diameter (≈4.34 Å) of the inner shell of Pt(4,4)@(11,11) is

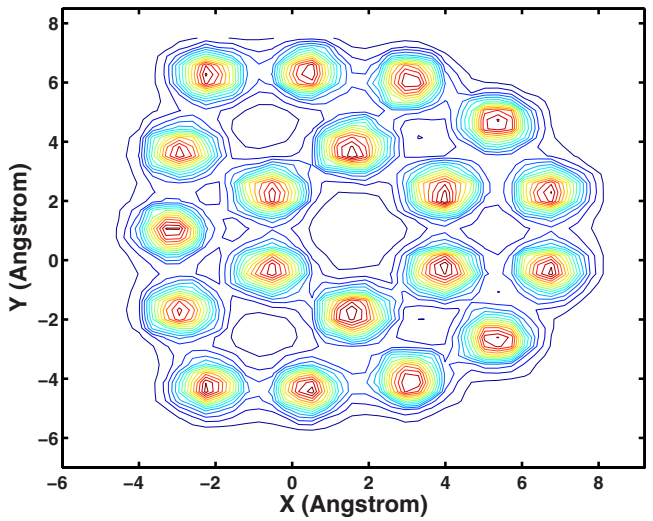

FIG. 15. (Color online) The total charge density plot of the Pt(6,6)@(13,13) nanotube on a plane perpendicular to the axis of the nanotube. The charge density is negligible at the center of the tube.

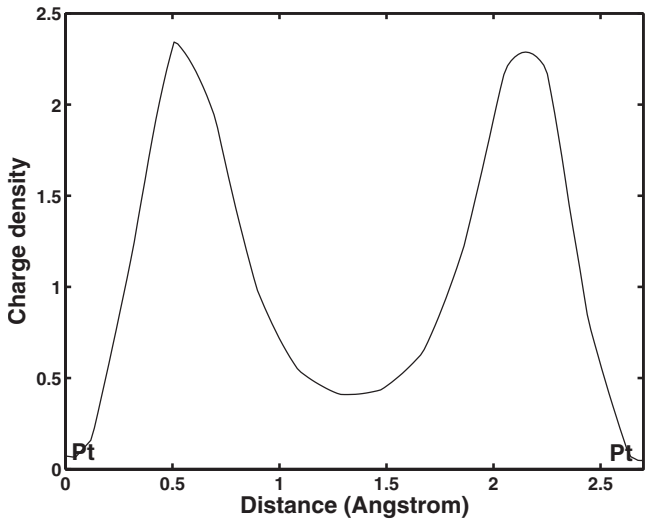

FIG. 16. The total charge density is plotted along a line between the two atoms, one in the inner shell and other in outer shell of the relaxed Pt(6,6)@(13,13) nanotube.

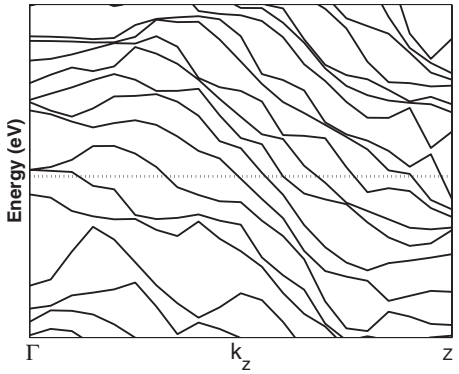

FIG. 17. The band structure plot of the relaxed Pt(6,6)@(13,13) nanotube. The dotted line indicates the fermi energy level.

more than the average diameter of the relaxed single-walled Pt(4,4) [≈3.47 Å].

Finally, we consider the HMS wire structure, where a straight chain is inserted within the Pt(7,7) tube. After complete relaxation, the results of average width and diameter of Pt(1,1)@(7,7) turns out to be ≈5.14 and ≈5.46 Å, respectively, which are almost close to the results obtained by Oshima *et al.*[38] The Pt-Pt bond lengths in the outer shell of the relaxed Pt(1,1)@(7,7) ranges from 2.60 to 2.76 Å while the straight Pt chain in the central channel of the Pt(7,7) takes the zigzag pattern with varying bond length between 2.60–2.62 Å. Note that among all the double-walled Pt nanotubes, the Pt(6,6)@(13,13) has larger string tension while the Pt(1,1)@(7,7) has lower string tension (see Fig. 6).

IV. SUMMARY

We have carried out the electronic structure calculations for different kinds of achiral and chiral single-walled platinum nanotubes, double-walled platinum nanotubes, and helical multishell wire structure under the formalism of density functional theory. The curvature energies of all the single-walled platinum nanotubes are calculated and it is found to obey the classical elasticity theory. The string tension analysis is done to understand the structural stability of the platinum nanotubes. The string tension analysis reveals that the Pt(6,4) is the most stable nanotube among the nanotubes with six row strands and Pt(5,3) is the most stable nanotube among the nanotubes with five row strands. The relaxed atomic structures of Pt(6,4) and Pt(5,3) belong to local minima in the string tension curve and hence correspond to magic structures. The Pt(6,4) and Pt(5,3) remain chiral after complete relaxation, however, the initial well-defined chirality is lost. With relevance to the recent experiments, the width and diameter of Pt(6,4) are calculated and they are compared with the existing experimental results.[38] After complete relaxation, most of all the single-walled platinum nanotubes become distorted from the original atomic structure, yet they remain hollow and tubular. However, the Pt(10,10) is one of the single-walled nanotubes which retains its tubular structure almost perfectly after complete relaxation. This kind of tube will be very useful for technological and medical purposes.[44] Therefore, further experiments should be carried out to see if under some conditions, Pt(10,10) could be obtained.

In the case of double-walled platinum nanotubes, Pt(6,6)@Pt(13,13), Pt(5,5)@Pt(12,12), Pt(4,4)@Pt(11,11), and Pt(1,1)@Pt(7,7) are studied here and they are found to retain the tubular structure after complete relaxation. Even both the shells are clearly distinguishable. The width and the diameter of Pt(6,6)@Pt(13,13) obtained from our calculations are compared with the existing experimental results.[38] Most of the results obtained from our calculations agree with the existing results.[38] Our results indicate that five row strands platinum nanotube may also be observed experimentally by peeling off the outer shell of Pt(5,5)@(12,12).

ACKNOWLEDGMENTS

One of the authors, B.C.G., is thankful to the Department of Physics, University of Illinois at Chicago for providing him with the local hospitality and for extending the research facilities during this work. Also, B.C.G. acknowledges the partial financial support from the CSIR funded Project No. 03(1081)/06/EMR-II, India

*shyam_konar@yahoo.co.in
†bikashc.gupta@visva-bharati.ac.in

[1] S. Iijima, Nature (London) **354**, 56 (1991); S. Iijima, and T. Ichihasi, *ibid.* **363**, 603 (1993).
[2] J. Cumings and A. Zettl, Chem. Phys. Lett. **316**, 211 (2000).
[3] Q. Wu, Z. Hu, X. Wang, Y. Lu, X. Chen, H. Xu, and Y. Chen, J. Am. Chem. Soc. **125**, 10176 (2003).
[4] J. Goldberger, R. He, Y. Zhang, S. Lee, H. Yan, Heon-Jin Choi, and P. Yang, Nature (London) **422**, 599 (2003).
[5] Y. R. Hacohen, E. Grunbaum, R. Tenne, J. Sloan, and J. L. Hutchison, Nature (London) **395**, 336 (1998).
[6] Q. Chen, W. Zhou, G. Du, and L. M. Peng, Adv. Mater. (Weinheim, Ger.) **14**, 1208 (2002).
[7] G. R. Patzke, F. Krumeich, and R. Nesper, Angew. Chem. Int. Ed. **41**, 2446 (2002).
[8] J. Sha, J. Niu, X. Ma, J. Xu, X. Zhang, Q. Yang, and D. Yang, Adv. Mater. (Weinheim, Ger.) **14**, 1219 (2002).
[9] X.-H. Sun, C.-P. Li, W.-K. Wong, N.-B. Wong, C.-S. Lee, S.-T. Lee, and J. A. Boon-Keng, J. Am. Chem. Soc. **124**, 14464 (2002).
[10] N. Keller, C. Pham-Huu, G. Ehret, V. Keller, and M. J. Ledoux, Carbon **41**, 2131 (2003).
[11] D. Östling, D. Tománek, and A. Rosén, Phys. Rev. B **55**, 13980 (1997).
[12] S. Reich, C. Thomsen, and P. Ordejón, Phys. Rev. B **65**, 155411 (2002).
[13] M. Menon, E. Richter, A. Mavrandonakis, G. Froudakis, and A. N. Andriotis, Phys. Rev. B **69**, 115322 (2004).

[14] K. M. Alam and A. K. Ray, Nanotechnology **18**, 495706 (2007).
[15] K. M. Alam and A. K. Ray, Phys. Rev. B **77**, 035436 (2008).
[16] G. Y. Gou, B. C. Pan, and L. Shi, Phys. Rev. B **76**, 155414 (2007).
[17] H. J. Xiang, J. Yang, J. G. Hou, and Q. Zhu, Phys. Rev. B **68**, 035427 (2003).
[18] E. Durgun, S. Tongay, and S. Ciraci, Phys. Rev. B **72**, 075420 (2005).
[19] G. Seifert, T. Köhler, K. H. Urbassek, E. Hernandez, and T. Frauenheim, Phys. Rev. B **63**, 193409 (2001).
[20] S. B. Fagan, R. J. Baierle, R. Mota, A. J. R. da Silva, and A. Fazzio, Phys. Rev. B **61**, 9994 (2000).
[21] B. Baumeier, P. Krüger, and J. Pollmann, Phys. Rev. B **76**, 085407 (2007).
[22] V. M. K. Bagci, O. Gülseren, T. Yildirim, Z. Gedik, and S. Ciraci, Phys. Rev. B **66**, 045409 (2002).
[23] E. Durgun, S. Dag, V. M. K. Bagci, O. Gülseren, T. Yildirim, and S. Ciraci, Phys. Rev. B **67**, 201401(R) (2003).
[24] A. K. Singh, T. M. Briere, V. Kumar, and Y. Kawazoe, Phys. Rev. Lett. **91**, 146802 (2003).
[25] J. K. Gimzewski and R. Möller, Phys. Rev. B **36**, 1284 (1987).
[26] S. Ciraci and E. Tekman, Phys. Rev. B **40**, 11969 (1989).
[27] N. Agrait, J. G. Rodrigo, and S. Vieira, Phys. Rev. B **47**, 12345 (1993).
[28] N. Agrait, G. Rubio, and S. Vieira, Phys. Rev. Lett. **74**, 3995 (1995).
[29] J. I. Pascual, J. Méndez, J. Gómez-Herrero, A. M. Baro, N. García, and V. T. Binh, Phys. Rev. Lett. **71**, 1852 (1993).
[30] H. Mehrez and S. Ciraci, Phys. Rev. B **56**, 12632 (1997).
[31] O. Gülseren, F. Ercolessi, and E. Tosatti, Phys. Rev. Lett. **80**, 3775 (1998).
[32] M. R. Sørensen, M. Brandbyge, and K. W. Jacobsen, Phys. Rev. B **57**, 3283 (1998).
[33] Y. Kondo and K. Takayanagi, Science **289**, 606 (2000).
[34] Y. Oshima, A. Onga, and K. Takayanagi, Phys. Rev. Lett. **91**, 205503 (2003).
[35] E. Tosatti, S. Prestipino, S. Kostlmeier, A. Dal Corso, and F. D. Di Tolla, Science **291**, 288 (2001).
[36] R. T. Senger, S. Dag, and S. Ciraci, Phys. Rev. Lett. **93**, 196807 (2004).
[37] S. L. Elizondo and J. W. Mintmire, Phys. Rev. B **73**, 045431 (2006).
[38] Y. Oshima, H. Koizumi, K. Mouri, H. Hirayama, K. Takayanagi, and Y. Kondo, Phys. Rev. B **65**, 121401(R) (2002).
[39] L. Xiao and L. Wang, Chem. Phys. Lett. **430**, 319 (2006).
[40] G. Kresse, and J. Hafner, Phys. Rev. B **47**, 558 (1993); **49**, 14251 (1994).
[41] G. Kresse and J. Furthmüller, Comput. Mater. Sci. **6**, 15 (1996).
[42] G. Kresse and J. Furthmuller, Phys. Rev. B **54**, 11169 (1996).
[43] G. Kresse and J. Hafner, J. Phys.: Condens. Matter **6**, 8245 (1994).
[44] A. J. Ciani, B. C. Gupta, and I. P. Batra, Solid State Commun. **147**, 146 (2008).
[45] V. M. García-Suárez, A. R. Rocha, S. W. Bailey, C. J. Lambert, S. Sanvito, and J. Ferrer, Phys. Rev. Lett. **95**, 256804 (2005).